Design and Analysis of Continuous Virus Inactivation Reactors in Biopharmaceutical Production

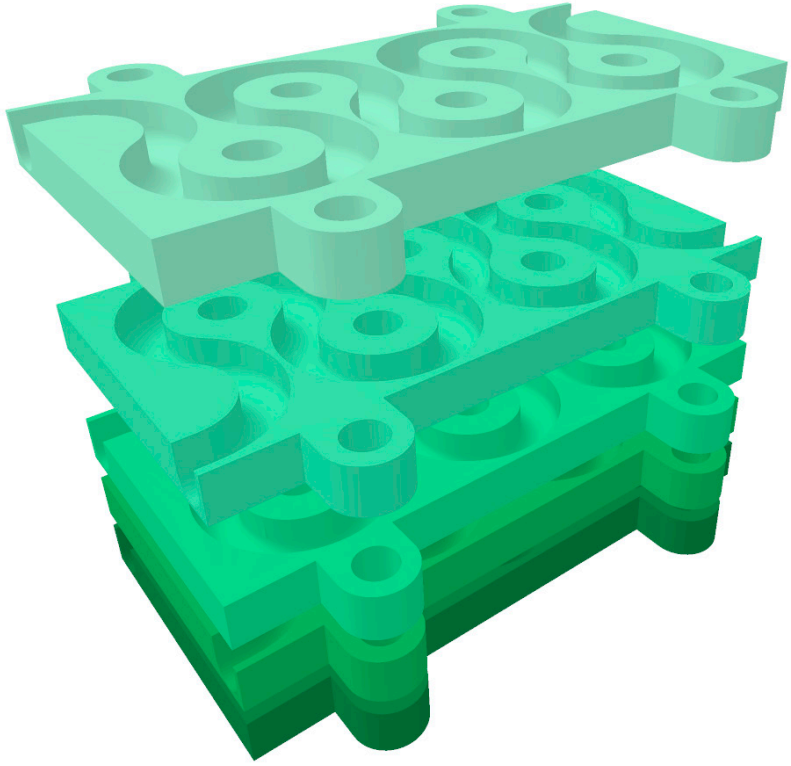

Hanna Danielsen

Department of Chemical Engineering
Master Thesis 2020

LUND UNIVERSITY

LUND UNIVERSITY

Master Thesis

Design and Analysis of Continuous Virus Inactivation Reactors in Biopharmaceutical Production

by

Hanna Danielsen

Department of Chemical Engineering
Lund University
Sweden
March 27, 2020

Supervisor: **Associate Senior Lecturer Niklas Andersson**
Examiner: **Professor Bernt Nilsson**

Postal address
PO-Box 124
SE-221 00 Lund, Sweden
Web address
www.lth.se/chemeng

Visiting address
Naturvetarvägen 14

Telephone
+46 46-222 82 85
+46 46-222 00 00

Printed in Sweden by Media-Tryck.
Lund 2020

Acknowledgements

I would like to thank everyone at the Department of Chemical Engineering for taking such good care of me, I really felt as a part of the department. It was a lot of fun being part of Bernt's research group. Thanks to everyone for the well-needed breaks, for the possibility to always ask anyone for help, and for all the support and encouragement you gave me. I would also like to thank Niklas, my supervisor, for all the help I've got during my master thesis.

I would also like to give a special thanks to my office buddy, Daniel, for spending hours discussing my thesis and helping me with my work. The final thank you goes to my family for always supporting me through my years of studying.

Thank You!

Abstract

The biopharmaceutical industry is replacing the current batch process with a continuous one and an essential step in the downstream process is the virus inactivation (VI). The challenge with a continuous VI reactor is to generate a narrow residence time distribution (RTD), while ensuring a precise incubation time. In this thesis, two different continuous virus inactivation reactors, the Jig In a Box (JIB) and a packed bed column, are designed and experimentally evaluated to determine which reactor is more suitable for a continuous production of antibodies. Pulse tracer tests are conducted to estimate the performance of the reactors. Both reactors generate a narrow RTD. For the JIB, however, the effect is highly dependent on the flow rate. The packed bed column performed better or equally to the JIB. Furthermore, the packed bed column is user friendly, has a much lower buffer consumption than the JIB and it is able to run at the low flow rates commonly used in antibody production. The packed bed column is, therefore, the better option for a continuous VI reactor for a production of antibodies.

Sammanfattning

Biofarmaindustrin håller på att byta ut de nuvarande satsvisa processerna mot kontinuerliga och ett viktigt steg i nedströmsprocessen är virusinaktiveringen. En utmaning med en kontinuerlig virusinaktivering är att genera en smal uppehållstidsfördelning samtidigt som man säkerställer en exakt inkubationstid. I den här masteuppsatsen designas och experimentellt utvärderas två virusinaktiveringsreaktorer för att avgöra vilken reaktor som är mer lämpad för en kontinuerlig produktion av antikroppar. Reaktorerna som testades är en "Jig In a Box"-reaktor (JIB) och en packad kolonnreaktor. Pulssvarsexperiment utfördes på reaktorerna för att bedöma deras prestanda. Experimenten visar att båda reaktorerna erhåller smala upphållstidsfördelningar, dock är bredden på upphållstidsfördelningen för JIB:en mycket beroende av flödet. Den packade kolonnen presterar bättre eller lika bra som JIB:en. Dessutom är den packade kolonnen användarvänlig, har en lägre buffertåtgång än JIB:en och den kan köras vid de låga flöden som oftast används vid antikroppstillverkning. Därför är den packade kolonnen är ett bättre alternativ som en virusinaktiveringsreaktor vid kontinuerlig produktion av antikroppar.

Table of Contents

1 Introduction

1.1 Overview

Purification is essential in production of biopharmaceuticals, for example antibodies and the downstream process is usually performed in batch as chromatography steps are involved. However, as the pharmaceutical industry is moving towards continuous production, the downstream processing has to follow (Gillespie et al., 2018). One step in some downstream processes is virus inactivation, and the conversion of this step to a continuous reactor remains a challenge (Martins et al., 2019). Safety is important when producing pharmaceuticals and a continuous inactivation reactor has to meet the same safety requirements as for the batch process. Commonly used methods for virus inactivation involve incubating the product in some kind of solution for a specific amount of time. The main safety concern with a continuous reactor is to ensure the whole product is subjected to the solution for the entire incubation time.

1.2 Aim

The aim of this thesis is to design and evaluate two different continuous virus inactivation reactors and determine which reactor is most suitable for continuous production of antibodies.

2 Background

The production of biopharmaceuticals is increasing and will continue to do so (Steinebach, Müller-Späth, & Morbidelli, 2016). This puts pressure on the downstream process of the production since it is well known that the downstream process is costly and an ineffective part of the production (Doelle et al., 2009). To handle this, the traditional batch-based downstream process is being replaced by a continuous one (Gillespie et al., 2018). The downstream process of antibodies typically include the following steps: capture chromatography, virus inactivation, polishing, viral filtration, UF/DF filtration, and formulation (Diefenbach-Streiber, Enzelberger, Kölln, Prassler, & Tesar, 2010; Steinebach et al., 2016). A major challenge is to design a continuous virus inactivation (VI) reactor (Martins et al., 2019) that meets the requirements of VI.

2.1 Virus Inactivation

As in any other production of pharmaceuticals, safety is important. For production of antibodies, the main safety concern is viruses, which is why the VI process is crucial (Shukla & Aranha, 2015). One method to accomplish VI is the low pH method. The idea of this method is to incubate the antibodies at a low pH, typically at a pH below 3.8, for 30 minutes or more to obtain a sufficient viral reduction (Orozco et al., 2017). Currently, the process is batch-based, and it is performed as follows: the eluted product from the primary capture step is transferred to a holding tank and the pH is lowered, then the solution is transferred to another tank where it is incubated for the 30 to 60 minutes. This is to handle the 'hanging drop problem', which means that you want to avoid droplets on the side or on the roof of tank, which have not been subjected to the low pH conditions. (Gillespie et al., 2018; Shukla & Aranha, 2015) Further, it is well known that long exposure to low pH causes aggregation of the antibodies, and these aggregates are considered as impurities (Mazzer, Perraud, Halley, O'Hara, & Bracewell, 2015). The incubation time can, therefore, not be too long.

Another method for VI is the solvent/detergent or detergent inactivation. The principle is the same as for the low pH method. However, this method is used on products that can not tolerate low pH (Shukla & Aranha, 2015). Even though the viruses are inactivated after a couple of minutes with this method, the incubation time is often a lot longer in manufacturing processes (Dichtelmüller et al., 2009).

2.2 Laminar Flow and Dispersion

There are a lot of challenges that have to be tackled when converting from a batch process to a continuous one. One of them is making sure the continuous VI reactor has a precise residence time to ensure total viral inactivation. The most basic incubation reactor would be a simple tube. However, in preparative chromatography the velocities can be low and using a simple tube would cause a lot of axial dispersion due to laminar flow. Laminar flow is present at low velocities, or more correctly at low Reynolds numbers, and it is characterised by smooth flow, in comparison with turbulent flow, which includes eddies and recirculation (Tavoularis, 2004). In a pipe or tube, a laminar flow causes a parabolic flow profile, called Poiseuille flow, (see Figure 2.1a); the highest velocity is present in the centre of the pipe and the lowest at the wall. In a ideal plug flow, a pulse would leave the reactor with the same concentration and same velocity as it entered. However, in a real pipe, because of the parabolic flow profile the pulse is subjected to different velocities and dispersion will appear, also know as Taylor dispersion (Gillespie et al., 2018; Orozco et al., 2017). This is demonstrated in Figure 2.1b.

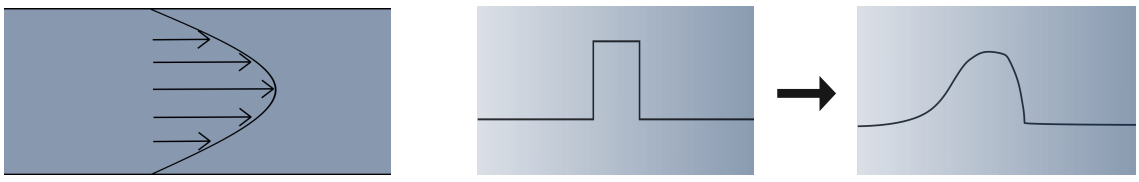

(a) **(b)**

Figure 2.1: (a) Laminar flow profile in a pipe. (b) Illustration of dispersion of a pulse.

2.3 Jig In a Box

As stated above, the axial dispersion is created by the laminar flow present in a straight tube, so any pulse or sample send into a pipe will spread out. One way to disrupt the laminar profile is by changing the path of the liquid, i.e. adding direction changes. In an article by Orozco et al. (2017), they did this by designing and 3D printing what they refer to as a Jig In a Box (JIB), and a schematic picture of their design is displayed in Figure 2.2. The purpose of the direction changes is to increase the radial mixing and minimise axial dispersion. The JIB's design was based on previously tested and evaluated VI reactors which revealed that the focus should be on maximising the numbers of bends and minimising the length of straight sections. Orozco et al. (2017) also state that the governing factor is not how these direction changes are formed but rather it is the number of them. The requirements for the JIB were to obtain a minimum residence time to be able to ensure viral inactivation, while also generating a narrow residence time distribution (RTD). Furthermore, the design should be scalable. The important design parameters and values for their design is displayed in Table 2.1.

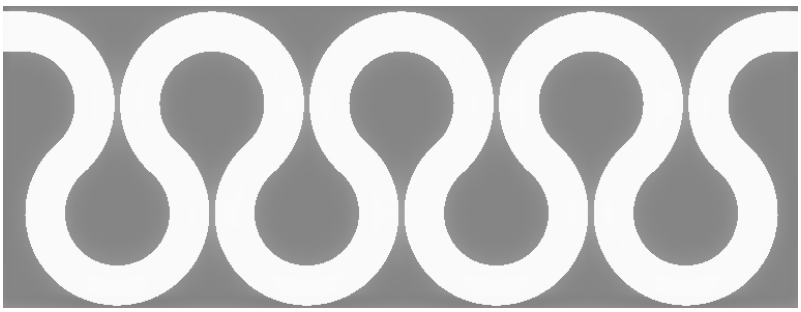

Figure 2.2: Illustration of the JIB by Orozco et al. (2017).

Table 2.1: Design parameters used by Orozco et al. (2017).

Inner diameter	0.635 cm
Radius of curvature	2.64 cm
Velocity	0.0526 m/s
Reynolds number	337
Channel length	16.44 m

According to Orozco et al. (2017), the JIB can accomplish a minimal residence time of 60 minutes and all the product has left the reactor after 75±3 minutes, i.e a narrow RTD. The JIB is robust and scalable, though an increase in length will generate a wider RTD. To quantify the RTD, they used the ratio of the time when 50 % and 0.5 % of a tracer had left the reactor and this ratio was about 1.06 for the setup found in Table 2.1. The reactor is not perfect since the radial mixing does not entirely eliminate the Taylor dispersion. In fact, Orozco et al. (2017) state that dispersion will always occur where there is laminar flow, and trying to improve the design will probably lead to small returns to the RTD. Even though the JIB is scalable, there is limitation to this scalability since the design is based on a secondary flow pattern. There is also a concern with the pressure drop along the reactor as the flow channel is both long and thin, this especially applies to if the JIB is made in a larger scale.

2.4 Packed Bed Reactor

Another possible continuous reactor that would generate a narrow RTD is the packed bed reactor. In contrast with the JIB, a packed bed does not rely on a secondary flow pattern which otherwise could cause problems with scale up (Martins et al., 2019). Martins et al. (2019) evaluated and compared a packed bed reactor with the current batch process. The packing consisted of non-porous beads with a diameter of 200-400 µm. They showed that this form of reactor had a RTD ratio, the ratio of the time when 50 % and 0.5 % of a tracer had left the reactor, between 1.1-1.3 and it is as efficient as the batch process. A significant advantage with a column, as in liquid chromatography, is that a scale up would generate an even better RTD. It is also easy to vary the incubation time by changing the flow rate. Moreover, packed beds are well know within the biopharmaceutical industry, meaning that a shift to a continuous packed bed reactor would be relatively easy. (Martins et al., 2019) A disadvantage with packed bed columns is that there is always a question with failure caused by the packing failing or channelling within the packing. There is also a concern with pressure drop across the column. However, since the packing consists of non-porous solid beads, there is a very low risk of both failure and large pressure drop. (Martins et al., 2019)

2.5 The Work in this Thesis

In this thesis, a JIB is designed and 3D printed using the design developed by Orozco et al. (2017) as the primary outset. The JIB is compared with a straight tube with the same length and diameter. In addition, simulations of the flow and how it is affected by the JIB is conducted. Further, a similar packed bed reactor as the one used by Martins et al. (2019) is created and tested in the lab. Finally, the results from the three setups are evaluated separately and together to be able to conclude which design is better.

3 Materials and Methods

The work of this thesis can be divided into three parts. The first part included designing the JIB in a 3D drawing programme and later 3D printing said design. Secondly, the fluid flow in the JIB was simulated and the effect was evaluated in comparison with a simple straight tube. Lastly, the three physical reactors, i.e. the JIB, the straight tube and the packed bed column, were tested in the lab to evaluate their performance.

3.1 Design and 3D printing of the JIB

The idea of the design was to use a tube and to 3D print a flow path where the tube could be placed. The first step of the 3D printing process was to draw and design the flow path. Firstly, the dimensions of the design had to be determined; some were calculated and others were results of physical restraints. The radius of curvature for the design was calculated using the ratio (f_{curve}) between the radius of curvature and the inner diameter for the JIB created by Orozco et al. (2017), see equation 3.1.

$$R_{curvature} = f_{curve} \cdot D_i \tag{3.1}$$

The design in this project differs from the one by Orozco et al. (2017) in that, instead of having a flow channel, a flow path was designed where a tube could be placed. The reason for this difference was that the 3D printer available was not able to print a watertight design. Since a path is constructed using the outer diameter of the tube, the bends would not be as snug as they could have been if a flow channel was printed directly. However, as stated before in section 2.3, it is the number of direction changes that is important, not the bend itself (Orozco et al., 2017).

The software used for the design and 3D drawing was OpenSCAD, which is a script-only based modelling software. It is not possible to interact with a specific part of the design or to change it by mouse interaction. It can only be altered by changing the parameters, in so OpenSCAD creates accurate model and designs. (OpenSCAD, 2020) An assortment of the parameters used for the design in OpenSCAD can be found in Table 3.1, for a full description of the design, see Appendix A.

Table 3.1: Parameters for the 3D drawing of the plate.

Channel width	1.1 cm
Radius of curvature	2.0 cm
Angle of bend	278°
Plate width	8.5 cm
Plate length	16.8 cm
Plate height	1.3 cm

The printer that was used was a Vertex K8400 from Velleman and the plastic was PLA. Since the 3D printer had a size constraint the flow path was divided into multiple sections, called plates. Each plate consisted of five whole bends with one half bend at each end. The plates were designed so they could be stacked on top of each other, in so the plate above acted as a lid to keep the tube in place. 'Feet' were added on each plate so later threaded rods could be used to keep the plates tightly together. Six plates were printed in total. A simple flat plate was also designed. Two of these flat plates were printed, one was used as a lid for the top plate and one was to be placed at the bottom to give stability to the construction when assembling the JIB.

The tube used for the JIB and the straight design was a Cole-Parmer Masterflex Tygon tubing size 15 with an inner diameter of 4.8 mm. Both designs were connected to a chromatography system, which was used to perform the experiments. The JIB was assembled by putting the tube in the 3D printed plates and then stacking the plates on top of each other. The straight tube was taped along the tables in the lab and had a large loop since it needed to be connected to the chromatography system again.

3.2 Pulse Tracer Test

To determine the performance of the VI-reactors, both the simulations and the physical ones, a pulse tracer test was done. This meant that a short pulse was sent into each reactor and the response was detected at the outlet. From the response, the residence time distribution function, $E(t)$, and the cumulative distribution function, $F(t)$, can be calculated, according to equations 3.2 and 3.3 respectively, where C is the response detected at the outlet. (Roberts, 2009)

$$E(t) = \frac{C(t)}{\int_0^\infty C(t)dt} \tag{3.2}$$

$$F(t) = \int_0^t E(t)dt \tag{3.3}$$

The performance of the reactors in this thesis is defined as the ratio $t[F_{0.5}]/t[F_{0.01}]$. For the ideal plug flow reactor the value of the ratio is 1. This means that the time when 50 % of a pulse has left the reactor is the same time as for 1 %. Furthermore, from the residence time distribution the mean residence time, t_{mean}, can also be calculated, according to equation 3.4. (Roberts, 2009)

$$t_{mean} = \int_0^\infty E(t) \cdot tdt \tag{3.4}$$

3.3 Simulation in COMSOL Multiphysics

The simulations were divided into two parts. The first part was to evaluate the effect on the laminar flow and the second was to perform a pulse tracer test on a design similar to the printed JIB. The program used for the simulations was COMSOL Multiphysics. COMSOL is a modelling and simulation software that uses the finite element method to solve mathematical models of different physical systems, such as electromagnetic, fluid flow and heat transfer modules (COMSOL INC., 2020). In this thesis, it was used to solve the fluid flow and the dispersion of a pulse.

3.3.1 Simple JIB Design and the Effect on the Laminar Profile

As a primary design, a simple JIB with 4 bends giving a total length of 38.7 cm was designed and evaluated in COMSOL Multiphysics. The JIB was designed as a 3D geometry, see Figure 3.1. A straight tube with the same length was also created, the geometry was a 2D axisymmetric geometry. The laminar flow was solved as a stationary study at four different flow rates for both designs, the flow rates can be found in Table 3.2 together with their corresponding Reynolds number (Re). The effect on the laminar flow was evaluated and compared with the flow in the straight tube.

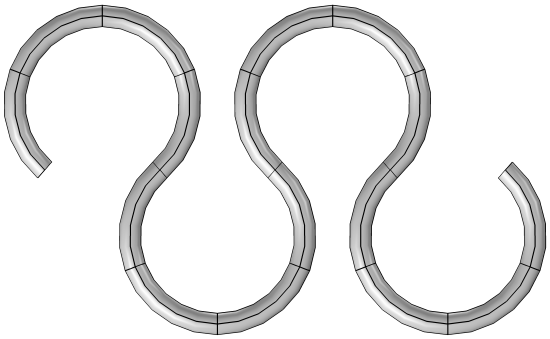

Figure 3.1: Simple JIB used in COMSOL Multiphysics.

Table 3.2: Flow rates and their corresponding Reynolds numbers for a pipe with a diameter of 4.8 mm and the kinematic viscosity for water at 20°C.

Flow rate (ml/min)	Reynolds number
5	22
10	44
15	66
20	88

3.3.2 Complex JIB and the Effect on a Pulse

To be able to make a good estimation of the printed JIB, the same geometry as the 3D printed one was created in COMSOL Multiphysics, see Figure 3.2. Because of the long simulation time, only a path with the length of two plates was created and

simulated. The total length of the simulated JIB was 138 cm. For this design, a pulse tracer test was conducted, which was done using a time dependent study. The laminar flow as a stationary study was first solved and the solution was used in the time dependent study. As for the simple JIB, a straight tube with the same length as the JIB was created and the same simulations were performed on it. The same flow rates as for the simulation of the simple design was used here, see Table 3.2.

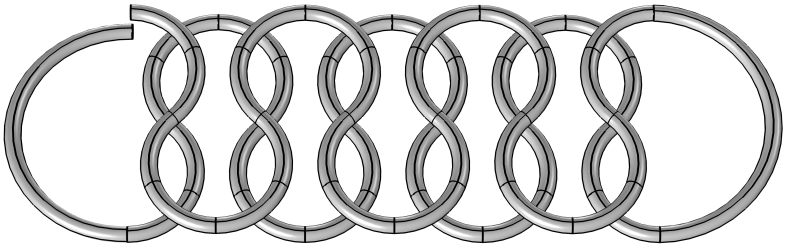

Figure 3.2: COMSOL Multiphysics design of the printed JIB.

3.4 Packed Bed Column

The packed bed reactor consisted of a column which later was packed with non-porous silica beads with a radius of $150-250$ µm. After the column was packed and connected to a chromatography system, a small pulse was injected into the column to determine the void volume. With the total volume (V_{total}) of the column and the void volume (V_{void}), the void (ε) was calculated, according to equation 3.5.

$$\varepsilon = \frac{V_{void}}{V_{total}} \tag{3.5}$$

Furthermore, the dispersion coefficient D_{sx} can be calculated according to equation 3.6, where r_p is the particle radius (here assumed to be 100 µm), v_{int} is the interstitial velocity and Pe_p is the Peclet number. The Peclet number is assumed to be 0.5.

$$D_{ax} = \frac{r_p \cdot v_{int}}{Pe_p} \tag{3.6}$$

3.5 Laboratory Work

The pulse tracer tests were mostly performed in the same way for all three setups. Water was used as a buffer and the pulse tracer consisted of 1 M sodium chloride and 0.2 g/l sodium fluorescein. Since the pulse response would be very dispersed, using a UV detector to measure the response was not an option and instead the conductivity was measured. The sodium fluorescein was only added as a visible agent to see the pulse as it travelled through the incubation rectors. The length of the pulse was 6 s for both the JIB and the straight tube, whereas for the packed bed reactor the length was 10 s.

For the JIB as well as the straight tube, the flow rates for which the pulse tracer tests were conducted ranged from 5 ml/min to 30 ml/min, with an interval of 5 ml/min. Since the volume of the column was not the same as the JIB's, it was decided that the mean residence time should be the same for the two. The JIB's mean residence times (t_{mean}) were calculated according to equation 3.7, where $t_{mean,\ exp}$ is the mean residence time calculated from the JIB experiments and $t_{dead\ volume}$ is the system's dead volume, such as tubing and valves.

$$t_{mean} = t_{mean,\ exp} - t_{dead\ volume} \tag{3.7}$$

The flow rates (F) for the packed bed column were calculated according to equation 3.8.

$$F = \frac{t_{mean}}{V_{void}} \tag{3.8}$$

4 Results and Discussion

In this chapter, the finished design and the printed version of the JIB are presented. The results for the simulations and the experiments on the three different reactors are presented and discussed. The results from the experiments on the straight tube and the JIB are evaluated together, since the same flow rates were used and they have the same volume. The packed bed column, on the other hand, is first reviewed by itself and then compared to the JIB.

4.1 Final Design of the 3D Printed JIB

The final 3D drawing of the plate and a printed one are displayed in Figure 4.1. The assembled JIB can be seen in Figure 4.2 and the total length of the tube was 409 cm with a volume of 74 ml.

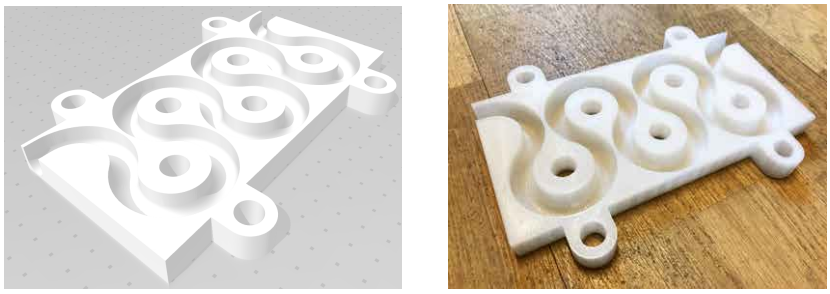

(a) **(b)**

Figure 4.1: (a) the 3D drawing of the designed plate and (b) the printed version.

Regarding the design, there are two main things that may be improved. Firstly, since a chromatography system was used to control the flow rate and inject the pulse, there was some capillary tubing involved. As the JIB consists of a tube with quite a large diameter, there needs to be a gradual expansion of the flow path when the liquid enters the JIB, and evidently a gradual reduction at the outlet. For this design, neither a gradual expansion nor reduction of the flow path are present. The lack of gradual expansion causes the pulse to not be injected in the properly. Secondly, the

tube used is flexible and can expand somewhat with increased pressure. This is not a major issue as long as the actual incubation time is observed.

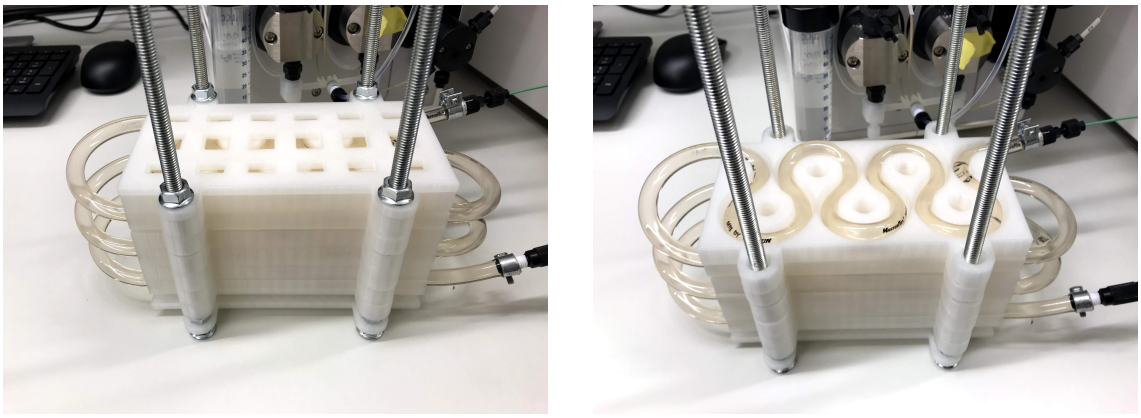

(a) **(b)**

Figure 4.2: Fully assembled JIB, (a) with and (b) without the top lid.

4.2 Simulations

4.2.1 Simple JIB Design and Velocity Evaluation

The simulations of the simple JIB design (see Figure 3.1 in section 3.1) shows that the effect of the JIB is immediate even at lower velocities in comparison with a straight tube. Figure 4.3 shows an overhead view of the flow path, it displays how the liquids velocity is affected along the JIB. The highest localised velocity occurs right after a direction change. Throughout a curve, the highest velocity is measured at the outer of the curve. This results in a thicker layer of liquid with a lower velocity at the inner part of the curve. When the flow path changes direction, the behaviour is the same. However, the liquid that was on the inside of the curve with a low velocity is now at the outside and has a higher velocity.

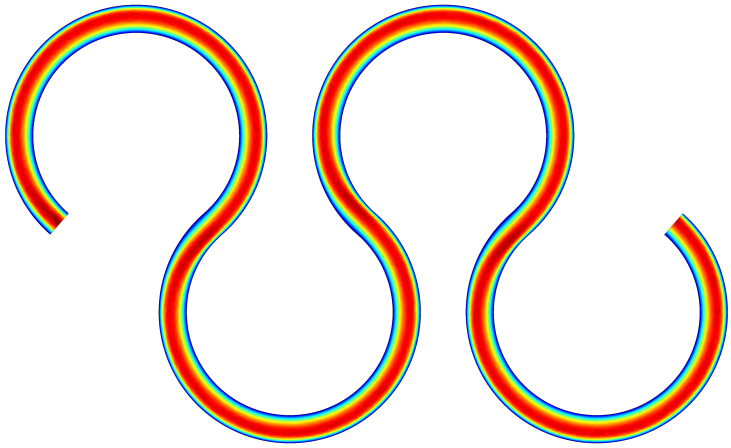

Figure 4.3: Overhead view of the velocity in the JIB.

In Figure 4.4, the axial velocity profile at two different positions in the JIB is displayed. Figure 4.4a is directly after the inlet and shows a typical laminar profile with the highest velocity in the middle which gradually decreases moving radially outwards. Figure 4.4b is at a latter part of a change in direction. Here the laminar profile is disrupted, the highest velocity is no longer in the centre of the pipe and the velocity is more even. This is also seen in Figure 4.5, which shows that the highest velocity is shifted towards the left or right, depending on which direction the tube is bent. This promotes radial mixing and decreases the axial dispersion which results in a narrower RTD if a pulse tracer test is conducted.

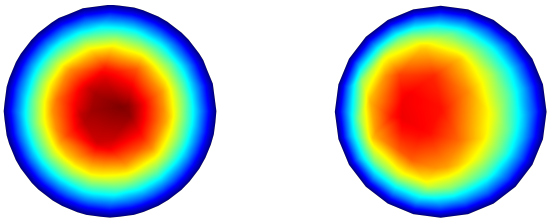

(a) **(b)**

Figure 4.4: Cross sections of the JIB showing the velocity at (a) the inlet and (b) at the end of a curve.

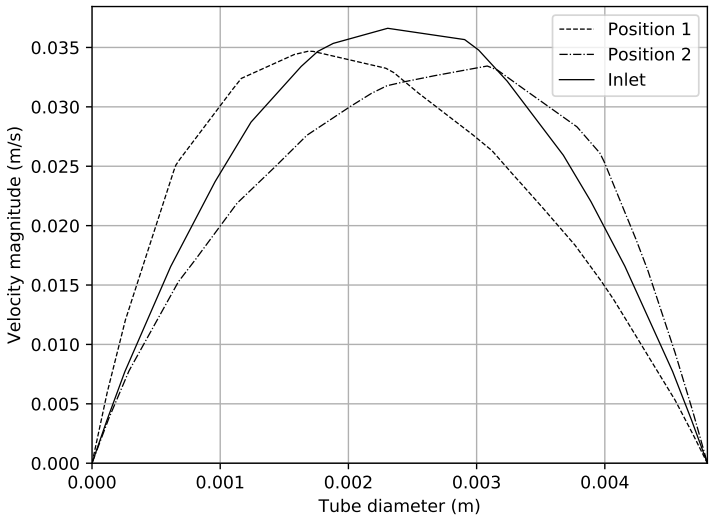

Figure 4.5: Radial velocity profiles in the middle of a 2D cross section at different positions along the JIB flow path.

4.2.2 Simulated Pulse Tracer Test

From the pulse tracer test conducted on the more complex designed JIB, which consisted of two plates (see Figure 3.2 in section 3.1), the effect on the RTD is visible for all the flow rates. At the lowest flow rate of 5 ml/min, there is a significant difference in the RTD, i.e. the width of the pulse peaks. For the JIB, the width is about 225 s whereas for the straight tube the width of the pulse response is about 380 s. This difference can be seen in Figure 4.6a and Figure 4.6c. This is expected since the liquid in the straight tube is experiencing a lot of Taylor dispersion. Increasing the velocity results in a narrower RTD for both the JIB and the straight tube. Figure 4.6b and 4.6d display the cumulative distribution function for the two setups.

$t[F_{0.5}]/t[F_{0.01}]$ and the mean residence times for the two setups at the different flow rates are displayed in Table 4.1. As described before in section 3.2, the value of $t[F_{0.5}]/t[F_{0.01}]$ shows how well the reactors are preforming in comparison to an ideal plug flow reactor. For the ideal plug flow reactor the value is 1, so a value close to 1 is desirable. The values of $t[F_{0.5}]/t[F_{0.01}]$ for the JIB and the straight tube are both decreasing with an increase in flow rate, which show a velocity dependent effect on the performance of the reactor.

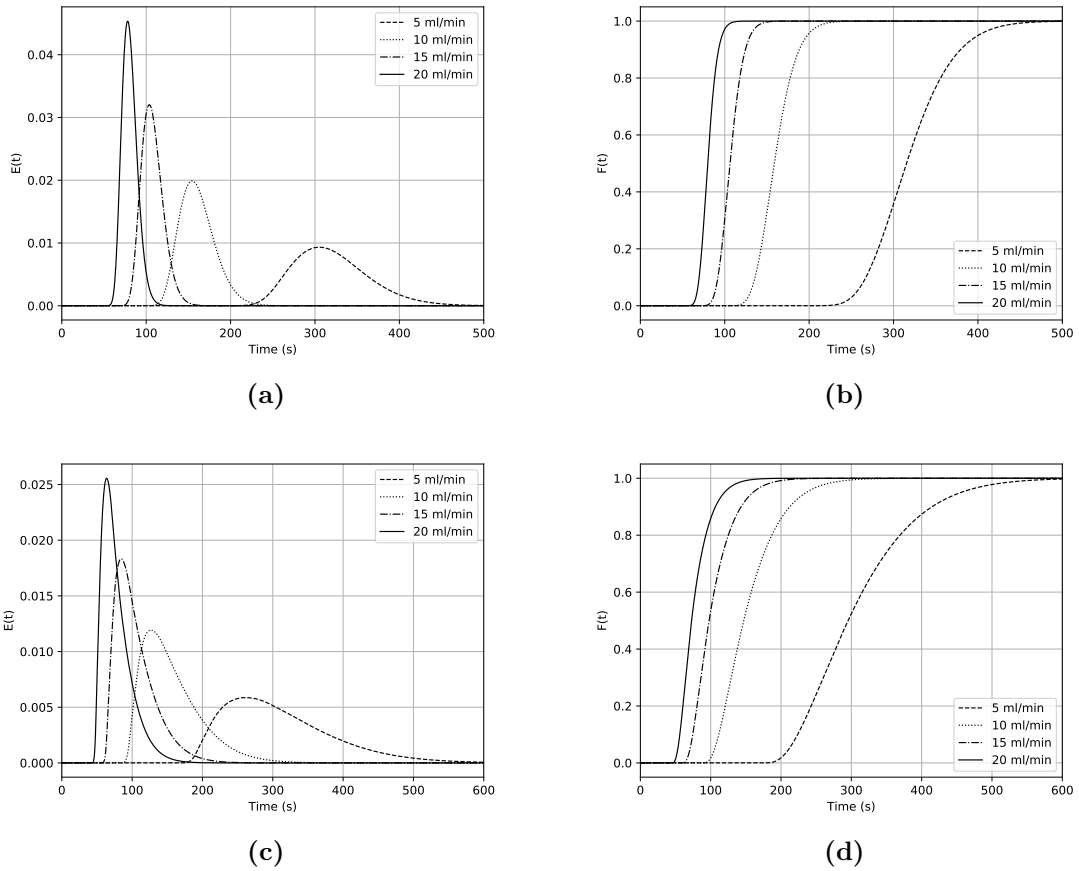

Figure 4.6: (a) the residence time distribution function $E(t)$ and (b) the cumulative distribution function $F(t)$ for the simulated pulse tracer test on the JIB. (c) the residence time distribution function and (d) the cumulative distribution function for the simulated pulse tracer test on the straight tube.

Table 4.1: The mean residence time, t_{mean}, and $t[F_{0.5}]/t[F_{0.01}]$ for different flow rates for the simulations of the JIB and the straight tube.

Flow rate (ml/min)	JIB		Straight tube	
	t_{mean} (s)	$t[F_{0.5}]/t[F_{0.01}]$	t_{mean} (s)	$t[F_{0.5}]/t[F_{0.01}]$
5	320	1.29	309	1.51
10	160	1.28	156	1.49
15	107	1.27	104	1.48
20	81	1.25	78	1.47

Overall, the JIB performs better than the straight tube. $t[F_{0.5}]/t[F_{0.01}]$ only includes the first part of the curve and as can be seen in Figure 4.6, the $E(t)$ curves for the straight tube show significant tailing and the width of the peaks are wider than the ones for the JIB. However, the total width of the peak is not taken into consideration with $t[F_{0.5}]/t[F_{0.01}]$, but it needs to be accounted for when designing and deciding on a virus inactivation reactor; otherwise this can become a problem, since a long incubation time will affect the productivity. Comparing the exit time of each flow rate, the pulse exits the JIB later than it does for the straight tube, i.e. the JIB has a longer residence time. This longer residence time means that a shorter tube is required to obtain the same residence time.

4.3 Experiments

4.3.1 JIB and Straight Tube

The results of four of the six flow rates for the JIB and straight tube are displayed in Figure 4.7. As in the simulations, the JIB has a narrower RTD overall, which results in a better performing reactor. There is one anomaly that needs to be addressed. The $E(t)$ curve at 10 ml/min for the JIB does not have the same shape as the other curves, the top of the peak is not as smooth as the others are. Multiple experiments with same flow rate of 10 ml/min and some surrounding flow rates was performed on the JIB to investigate what the source of the irregularity was and also if the irregularity was a one time occurrence or if it was systematic. The irregularity appeared for each of the test with the flow of 10 ml/min and it disappeared with an increase or decrease of the flow rate. One possible reason for this behaviour could be that the system ends up in some kind of self-induced oscillation, but this is only speculation. The multiple tests at the specific flow rate gave almost identical results, in both shape and mean residence time, and this repeatability suggests that the design is robust and performs consistently.

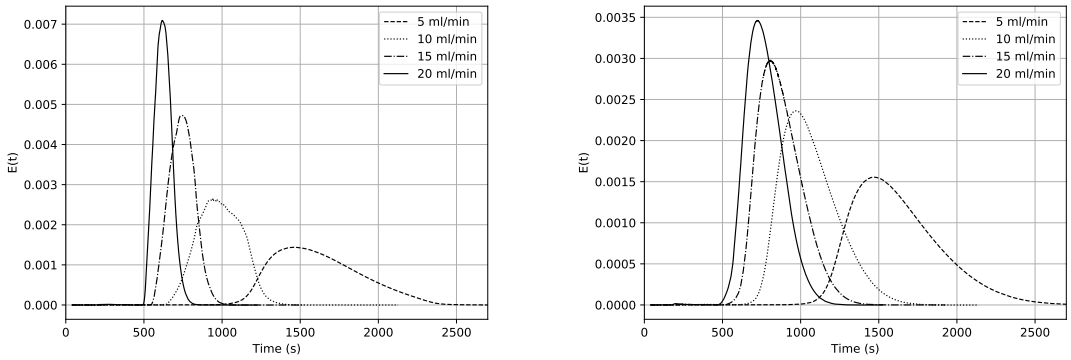

(a) **(b)**

Figure 4.7: The residence time distribution function $E(t)$ for the experimental pulse tracer test on (a) the 3D printed JIB and (b) the straight tube.

For an easier comparison of the JIB and the straight tube the $E(t)$ and $F(t)$ curves for three flow rates are displayed in 4.8 for both the JIB and the straight tube. At a flow rate 5 ml/ml there is little to no difference between the two, however an increase of the flow rate quickly affects the pulse response.

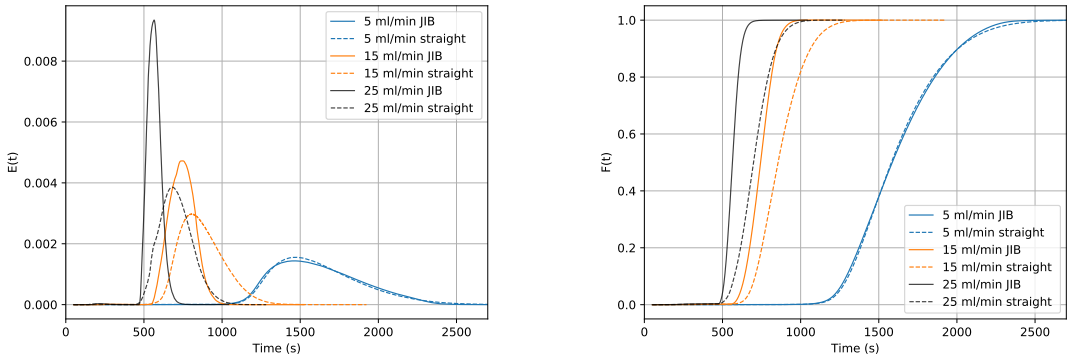

(a) **(b)**

Figure 4.8: (a) the residence time distribution function $E(t)$ and (b) the cumulative distribution function $F(t)$ for both the JIB and the straight tube.

The JIB's and the straight tube's mean residence time and $t[F_{0.5}]/t[F_{0.01}]$ are displayed in Table 4.2. $t[F_{0.5}]/t[F_{0.01}]$ for the straight tube is not decreasing, with the exception for the last flow rate of 30 ml/min. The JIB on the other hand, has about the same value at 5 and 10 ml/min and then it starts to decrease. As stated in section 3.2, the performance of a reactor is defined as the ratio between the time when 50% and the time when 1% of the tracer has exited the reactor. After observing the pulse response curves, it was decided that the latter part of the curve

would give important information as well, therefore both were studied. In Figure 4.9 $t[F_i]/t[F_{0.01}]$ of the reactors are displayed as a function of the flow rate. Q is defined as $t[F_i]/t[F_{0.01}]$ where i is either 0.5 or 0.99. For both the designs, $t[F_{0.99}]/t[F_{0.01}]$ is dependent on the flow rate, and overall the JIB has lower, i.e. better, value at any given flow rate and the value is decreasing more rapidly in comparison to the straight tube.

Table 4.2: The mean residence time, t_{mean}, and $t[F_{0.5}]/t[F_{0.01}]$ at different flow rates for the experiments of the JIB and the straight tube.

Flow rate (ml/min)	JIB		Straight tube	
	t_{mean} (s)	$t[F_{0.5}]/t[F_{0.01}]$	t_{mean} (s)	$t[F_{0.5}]/t[F_{0.01}]$
5	1612	1.39	1615	1.37
10	982	1.39	1057	1.38
15	741	1.28	870	1.37
20	621	1.20	769	1.38
25	564	1.16	704	1.38
30	527	1.12	645	1.35

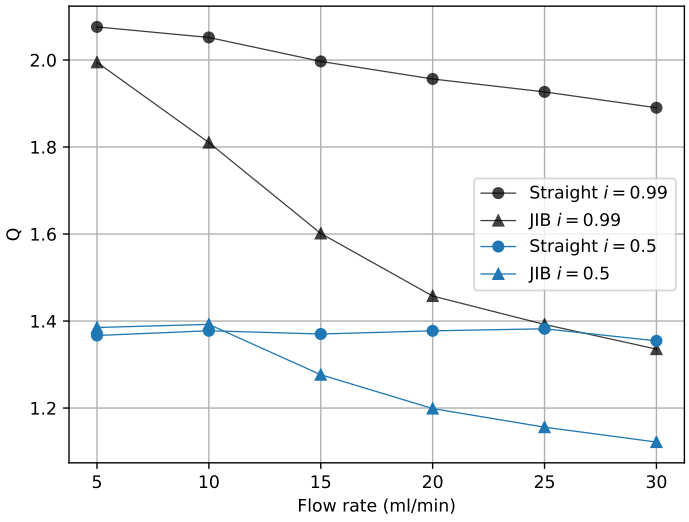

Figure 4.9: The ratio, Q, versus the flow rate. Q is defined as $t[F_i]/t[F_{0.01}]$ where i is either 0.5 or 0.99.

To summarise, for the straight tube the first half of the pulse response is not affected by a change in velocity, but the latter half is. In comparison, the whole pulse of the JIB is considerably affected by a velocity change.

As the performance is not affected by the length, the results from the simulations and the experiments can be compared. The experimental values for $t[F_{0.5}]/t[F_{0.01}]$ are more widely scattered, starting at 1.39 and going as low as 1.12. The simulation had values between 1.29 and 1.25. The simulations also suggest that the pulse should exit the JIB later than for the straight tube. This is not the case for the experiments; the pulse tracer is leaving the JIB earlier than in the straight tube, see Table 4.3. Table 4.3 also displays time for when 99 % of the tracer has left the reactor. The JIB has a much narrower RTD, for example at 20 ml/min the width is about 240 s which is more than half of the width for the straight tube. This means that for a flow rate of 20 ml/min, the residence time is about 8.5 min (518 s) and 99 % has left the JIB after about 12.5 min (755 s).

Table 4.3: Residence times (RT) and the time when 99 % of the tracer has left the reactor for the experimental pulse tracer tests.

Flow rate (ml/min)	JIB		Straight tube	
	RT (s)	99 % out (s)	RT (s)	99 % out (s)
5	1144	2287	1156	2400
10	705	1281	752	1543
15	582	931	624	1246
20	518	755	551	1078
25	487	678	505	973
30	468	625	474	896

4.3.2 Packed Bed Column

A picture of the packed bed column used in the experiments is displayed in Figure 4.10. The specifications for the packed bed column can be found in Table 4.4, the void volume was measured to 20.8 ml and with this value the flow rates were calculated, these can be found in Table 4.6. The dispersion coefficient for is displayed in Table 4.5.

Figure 4.10: Packed bed column.

Table 4.4: Specification of the packed bed column.

Void volume (V_{void})	20.8 ml
Total volume (V_{total})	45.7 ml
Void (ε)	0.46
Diameter	2.5 cm
Height	9.3 cm

Table 4.5: Dispersion coefficient for the packed bed column.

Flow rate (ml/min)	D_{ax} (m^2/s)
0.77	$1.15 \cdot 10^{-8}$
1.27	$1.89 \cdot 10^{-8}$
1.68	$2.70 \cdot 10^{-8}$
2.01	$3.23 \cdot 10^{-8}$
2.21	$3.55 \cdot 10^{-8}$
2.37	$3.80 \cdot 10^{-8}$

The $E(t)$ and $F(t)$ curves for the four lower flow rates from the pulse tracer tests conducted on the packed bed column are displayed in Figure 4.11. The $E(t)$ curves are looking a bit strange, it almost looks like there are two peaks for each flow rate. Multiple pulse tracer tests were conducted without any significant improvement. Despite this, the peaks are quite symmetrical overall, which is also visible in the $F(t)$ curves.

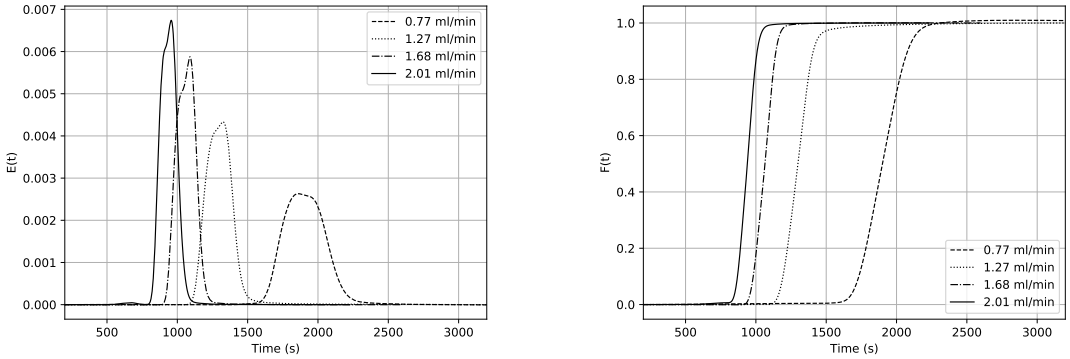

(a) **(b)**

Figure 4.11: (a) the residence time distribution function $E(t)$ and (b) the cumulative distribution function $F(t)$ from the pulse tracer test on the packed bed column.

There were issues with the conductivity measurements during experiments on the column, which caused problems when processing the data. This can be seen in the cumulative distribution curves, as some of the curves are going above 1 and the $F(t)$ curves should only have values between 0 and 1. $t[F_{0.5}]/t[F_{0.01}]$ and $t[F_{0.99}]/t[F_{0.01}]$ values and the mean residence times are found in the same table as the flow rates, Table 4.6. $t[F_{0.5}]/t[F_{0.01}]$ is about 1.13 for almost all of the flow rates, only the value for the flow rate 0.77 ml/min differs for the others. If instead $t[F_{0.99}]/t[F_{0.01}]$ is considered, there seems to be a trend around 1.30. These values suggest that the RTD is not dependent on the flow rate.

The mean residence times are longer than the ones attained for the JIB. The mean residence time should be the same since the flow rates for the packed bed column were calculated from the mean residence time obtained in the JIB. This makes it a bit more difficult to compare the results. However, since the mean residence times are within the same range, some comparison can be made. In Table 4.6, the residence time and the time for when 99 % of the tracer has left the column can also be found.

At the highest flow rate 2.37 ml/min the residence time is about 755 s which is almost the same as the residence time at 10 ml/min for the JIB (RT = 705 s). 99 % of tracer leaves the packed bed column after 967 s, resulting in a RTD of 212 s. For the JIB, on the other hand, the RTD is 576 s which is a significant difference.

Table 4.6: $t[F_{0.5}]/t[F_{0.01}]$, $t[F_{0.99}]/t[F_{0.01}]$, and the mean residence time for the pulse tracer tests performed on the packed bed column. Also the residence time (RT) and the time when 99 % of the tracer has left the packed bed column.

Flow rate (ml/min)	t_{mean} (s)	$t[F_{0.5}]/t[F_{0.01}]$	$t[F_{0.99}]/t[F_{0.01}]$	RT (s)	99 % out
0.77	1834	1.18	1.37	1614	2216
1.27	1278	1.14	1.58	1136	1795
1.68	1041	1.13	1.29	939	1216
2.01	920	1.14	1.31	824	1080
2.21	873	1.12	1.30	792	1029
2.37	832	1.12	1.29	755	967

5 Conclusion

Two different continuous virus inactivation reactors were designed and evaluated. The JIB was created by using a tube and 3D printed plates to place the tube in. The effect of the JIB on the RTD are present at most of the flow rates, the RTD is narrower and there is less tailing than if a simple straight tube were to be used. The printed JIB works, however, not as the simulations suggested. The physical JIB performed better than the simulations at the higher flow rates but, at lower flow rates the JIB did not perform as well. The physical JIB generates a narrower RTD and a has better performance than a simple straight tube but the effect of the JIB was visible at low flow rates. The JIB is robust and it is relatively easy to operate. However, it is difficult to adapt if the running conditions, such as flow rate and incubation time, need to be changed.

The other reactor, the packed bed column, is able to operate at lower flow rates and still obtain good results. In general, the packed bed generated a $t[F_{0.5}]/t[F_{0.01}]$ value of about 1.13 which is better or equal to what was obtained by the JIB. The packed bed column is more user friendly and less time consuming when setting up and preparing compared to the JIB. The packed bed column does not require hours or even days of printing and assembling the reactor as the JIB does, only a column and glass beads are needed. Furthermore, the performance of the packed bed column does not seem to be dependent on the flow rate which is useful if the running conditions are changed. A significant difference between the two reactors is the buffer consumption. As the flow rates are higher for the JIB and the residence times are about the same for the JIB and the packed bed column, the amount of buffer used is much higher for the JIB. The JIB uses somewhere between 250 and 400 ml of buffer per run, whereas the packed bed reactor uses about a tenth of that.

Since the packed bed column works for lower flow rates and has a similar or better performance than the JIB, the packed bed column would be the better option for a continuous VI reactor in an antibody purification process.

6 Future Work

If the JIB is to be used, the design needs to be developed and adapted to the specific flow rate, and the inlet and outlet have to be improved. However, spending this time on developing the packed bed column instead would be more useful and yield better results. More pulse tracer tests need to be conducted on the packed bed column to confirm the results and its effect on the RTD, as there was issues with the measurements performed on the packed bed column. The pulse tracer solution should have a higher concentration of the measured component so higher peaks can be obtained, which would give less problems with noise. The packed bed column should be tested with antibodies using both the low pH method and the solvent/detergent method. As a final step, the column should be connected to an existing antibody purification process.

References

COMSOL INC. (2020). Comsol: Multiphysics software for optimizing designs. Retrieved from https://www.comsol.se/. (accessed: 03.16.2020)

Dichtelmüller, H., Biesert, L., Fabbrizzi, F., Gajardo, R., Gröner, A., Hoegen, I., ... Poelsler, G. (2009). Robustness of solvent/detergent treatment of plasma derivatives: A data collection from Plasma Protein Therapeutics Association member companies. *Transfusion*, *49*, 1931–43. doi:10.1111/j.1537-2995.2009.02222.x

Diefenbach-Streiber, B., Enzelberger, M., Kölln, J., Prassler, J., & Tesar, M. (2010). Monoclonal Antibodies. In *Ullmann's Encyclopedia of Industrial Chemistry*. doi:10.1002/14356007.a16_699.pub2. eprint: https://onlinelibrary.wiley.com/doi/pdf/10.1002/14356007.a16_699.pub2

Doelle, H. W., Fiechter, A., Schlegel, G., Shimizu, S., Ulber, R., & Yamada, H. (2009). Biotechnology, 4. Downstream Processing. In *Ullmann's Encyclopedia of Industrial Chemistry*. doi:10.1002/14356007.n04_n04. eprint: https://onlinelibrary.wiley.com/doi/pdf/10.1002/14356007.n04_n04

Gillespie, C., Holstein, M., Mullin, L., Cotoni, K., Tuccelli, R., Caulmare, J., & Greenhalgh, P. (2018). Continuous In-Line Virus Inactivation for Next Generation Bioprocessing. *Biotechnology Journal*, *14*, 1700718. doi:10.1002/biot.201700718

Martins, D., Sencar, J., Hammerschmidt, N., Tille, B., Kinderman, J., Kreil, T., & Jungbauer, A. (2019). Continuous Solvent/Detergent Virus Inactivation Using a Packed-Bed Reactor. *Biotechnology Journal*, *14*. doi:10.1002/biot.201800646

Mazzer, A., Perraud, X., Halley, J., O'Hara, J., & Bracewell, D. (2015). Protein A chromatography increases monoclonal antibody aggregation rate during subsequent low pH virus inactivation hold. *Journal of chromatography. A*, *1415*. doi:10.1016/j.chroma.2015.08.068

OpenSCAD. (2020). Openscad.org. Retrieved from https://www.openscad.org/. (accessed: 03.16.2020)

Orozco, R., Amarikwa, L., Parker, S., Godfrey, S., Hernandez, L., Wachuku, C., ... Coffman, J. (2017). Design, construction, and optimization of a novel, modular, and scalable incubation chamber for continuous viral inactivation. *Biotechnology Progress*, *33*. doi:10.1002/btpr.2442

Roberts, G. W. (2009). Chemical Reactions and Chemical Reactors. (Chap. 10. Nonideal Reactors). John Wiley & Sons.

Shukla, A., & Aranha, H. (2015). Viral clearance for biopharmaceutical downstream processes. *Pharmaceutical Bioprocessing*, *3*, 127–138. doi:10.4155/pbp.14.62

Steinebach, F., Müller-Späth, T., & Morbidelli, M. (2016). Continuous countercurrent chromatography for capture and polishing steps in biopharmaceutical production. *Biotechnology Journal*, *11*(9), 1126–1141. doi:10.1002/biot.

201500354. eprint: https://onlinelibrary.wiley.com/doi/pdf/10.1002/biot.201500354

Tavoularis, S. (2004). Fluid Mechanics. In *Kirk-Othmer Encyclopedia of Chemical Technology*. doi:10.1002/0471238961.06122109191514.a01.pub2. eprint: https://onlinelibrary.wiley.com/doi/pdf/10.1002/0471238961.06122109191514.a01.pub2

A OpenSCAD script

```
/*
Hanna Danielsen, 2020
*/

\$fn = 20; //Resolution

kvot = 2.64/0.635;
di = 4.8; //Inner diameter tube
dy = 10+1; //Outer diameter tube
rc = kvot*di; //Radius curve
vinkel = 82; //Angle 278
dtot = 2*sin(vinkel/2)*rc; //The circles movement in x from the
    previous circle
ybredd = cos(vinkel/2)*rc; //The circles location from the y-axis
n = 6; //number of bends minus 1, has to be an even number

module boj() {
    translate([0, ybredd-0.001, 0])
        rotate([0, 0, -(45-(vinkel-90)/2)])
            rotate_extrude(angle=360-vinkel, convexity=10)
                translate([rc, 0, 0])
                    circle(d = dy);
}

module bojar(n){
    difference(){
        for(i = [0:n]){
        if((i % 2) == 0){
            rotate([0, 0, 0])
                translate([i*dtot, 0, 0])
                    boj();
            }
        else {
            rotate([180, 0, 0])
                translate([i*dtot, 0, 0])
```

```
35                      boj();
36              }
37          }
38
39
40      translate([-60, -10, -30])
41          cube(60);
42
43      translate([dtot*n, -10, -30])
44          cube(60);
45          }
46
47      translate([0.01, rc+ybredd-0.001, 0])
48          rotate([0, -90, 0])
49              cylinder(d=dy, h=50);
50
51      translate([n*dtot-0.01, rc+ybredd-0.001, 0])
52          rotate([0, 90, 0])
53              cylinder(d=dy, h=50);
54
55  }
56
57  module fot() {
58      translate([-20/2, 0, -(dy+2)/2])
59          difference(){
60              union(){
61                  cube([20, 10, dy+2]);
62                  translate([20/2, 0, 0])
63                      cylinder(d=20, h=dy+2);
64              }
65          translate([20/2, 0, -5])
66          cylinder(d=11, h=50);
67          }
68  }
69
70  translate([dtot, -(ybredd+rc+dy/2+1+10), 0])
71      fot();
72
73  translate([(n-1)*dtot, -(ybredd+rc+dy/2+1+10), 0])
74      fot();
75
76  translate([dtot, (ybredd+rc+dy/2+1+10), 0])
```

```
77      rotate(180)
78          fot();
79
80
81  translate([(n-1)*dtot, (ybredd+rc+dy/2+1 +10), 0])
82      rotate(180)
83          fot();
84
85  difference(){
86      translate([-(dtot/2-7.5), -(ybredd+rc+dy/2+2), -(dy+2)/2])
87          cube([(n+1)*dtot-15, 2*(ybredd+rc+dy/2+2), dy+2]);
88
89      linear_extrude(height=50)
90          projection()
91              bojar(n);
92
93      bojar(n);
94
95      translate([dtot, -(ybredd-0.001), -10])
96          cylinder(d=12, h=50);
97
98      translate([2*dtot, (ybredd-0.001), -10])
99          cylinder(d=12, h=50);
100
101     translate([3*dtot, -(ybredd-0.001), -10])
102         cylinder(d=12, h=50);
103
104     translate([4*dtot, (ybredd-0.001), -10])
105         cylinder(d=12, h=50);
106
107     translate([(n-1)*dtot, -(ybredd-0.001), -10])
108         cylinder(d=12, h=50);
109 }
```